

Sputtering and D retention properties of RAFM steels under high-flux plasma exposure

D. Nishijima, R.P. Doerner, M.J. Baldwin

Center for Energy Research, University of California - San Diego, La Jolla, CA, USA

1. Sputtering properties of RAFM steels

- First experimental determination of S/XB values of Fe I and Cr I lines
- Time evolution of element-resolved sputtered flux
- Temperature dependence of sputtering yield
- Surface morphology development

2. D retention properties of RAFM steels (preliminary)

- Comparison between CLF-1, Eurofer, and F82H

3. LIBS thickness measurement of (Fe, Cr, Ni) mixed-material layers

- New technique developed for layers thinner than ablation rate
- Simultaneous composition analysis

Optical emission spectroscopy can provide element-resolved sputtered flux and sputtering yield.

- ◆ Line-of-sight integrated emission intensity of sputtered atoms, I_a , can be converted into sputtered atomic flux, Γ_{spt} , with S/XB defined by,

$$G_{spt} = 4\rho \frac{S}{XB} I_a$$

S: Ionization rate coefficient
X: Excitation rate coefficient
B: Branching ratio

(Note that *this relation is valid only when the geometrical loss flux from the observation volume is negligible.*)

Availability of S/XB for main elements in RAFM steel

	Fe I	Cr I	W I
Experimental S/XB	N/A	N/A	Available
Theoretical S/XB	N/A	Available	Available

S/XB values of Fe I and Cr I lines were experimentally determined for the first time.

$$G_{spt} = 4\rho \frac{S}{XB} I_a \quad \rightarrow \quad \frac{S}{XB} = \frac{G_{spt}}{4\rho I_a} = \frac{Y\Gamma_i}{4\rho I_a}$$

Y: Sputtering yield from mass loss measurement
 Γ_i : Ion flux from single probe measurement

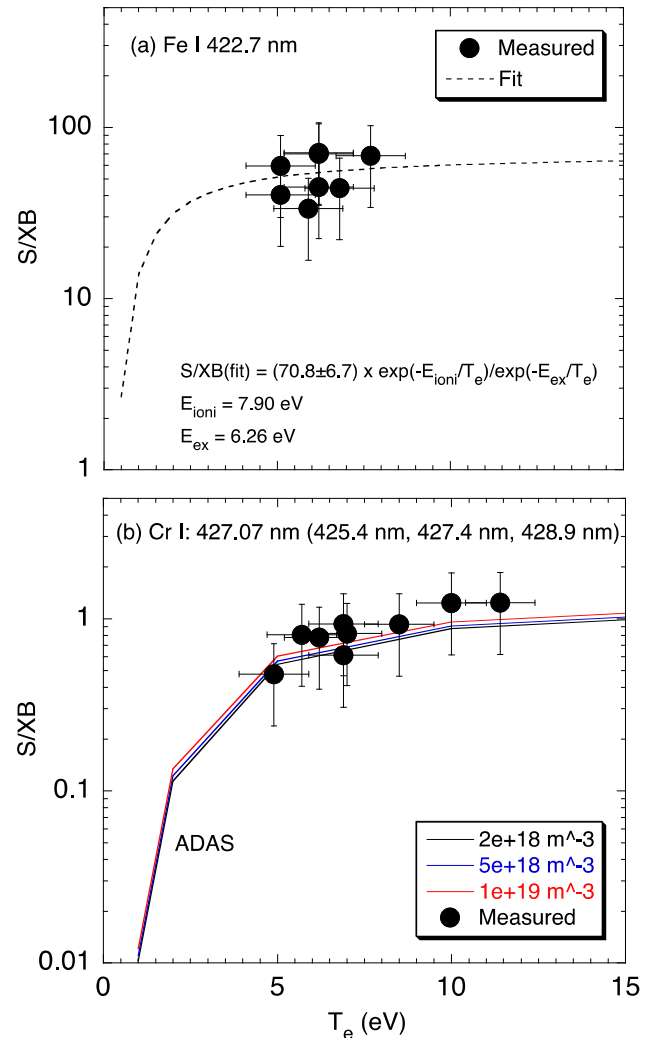
◆ Fe I 422.7 nm

- No theoretical data is available
- Fit to a simple function:

$$\frac{S}{XB} = b \times \exp\left(-\frac{E_{ioni}}{T_e}\right) / \exp\left(-\frac{E_{ex}}{T_e}\right)$$

◆ Cr I 427.07 nm (425.4, 427.4, 428.9 nm)

- A multiplet-averaged line
- Good agreement with ADAS



Reduction of sputtering yield of Fe and Cr due to He plasma exposure is clearly observed.

◆ He plasma exposure

- $\Gamma_i \sim (2-4) \times 10^{22} \text{ m}^{-2} \text{ s}^{-1}$
- $E_i \sim 80 \text{ eV}$

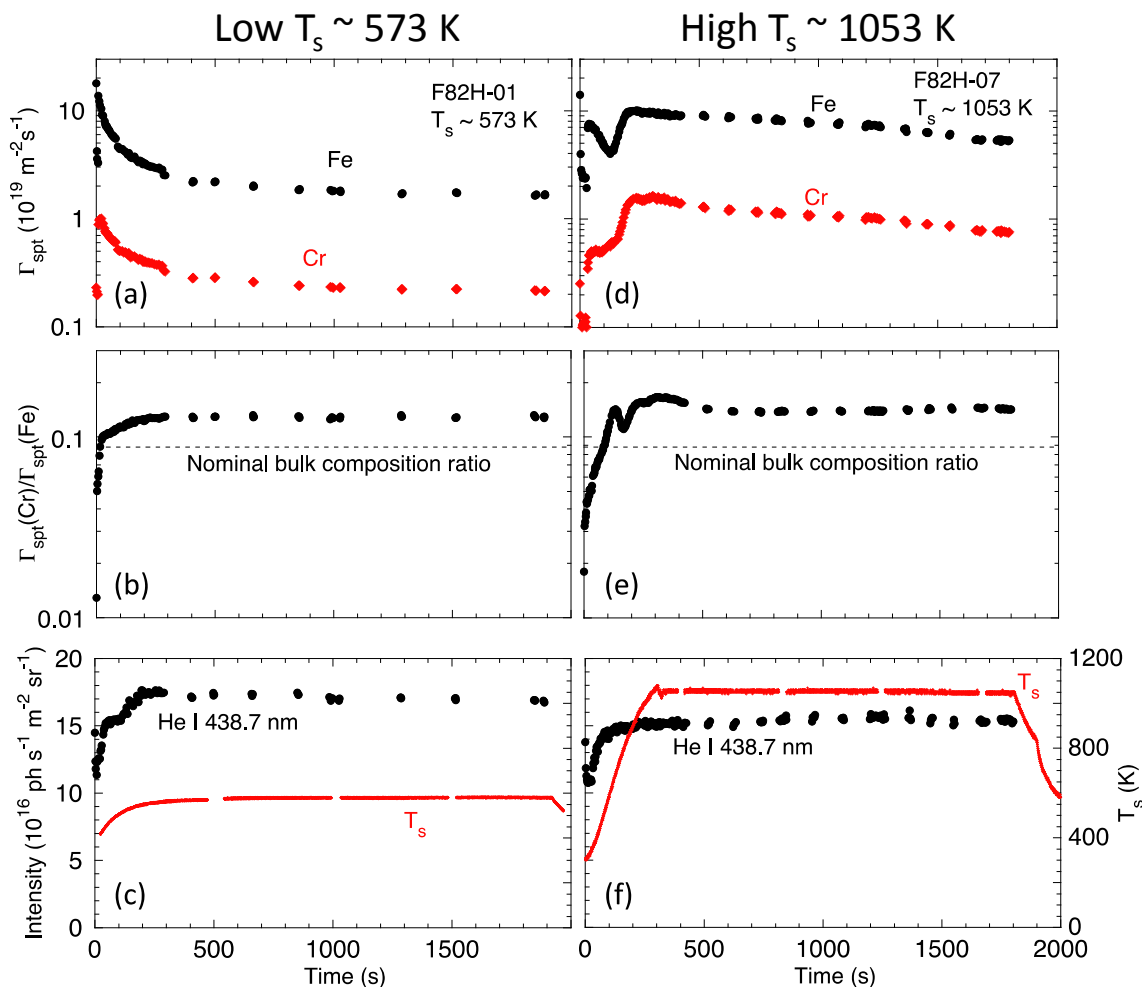
◆ No W I lines were observed.

- W was not sputtered.
- Preferential sputtering of Fe and Cr.

◆ Decay of $\Gamma_{\text{spt}}(\text{Fe})$ and $\Gamma_{\text{spt}}(\text{Cr})$ is faster at $T_s \sim 573 \text{ K}$ than at $T_s \sim 1053 \text{ K}$.

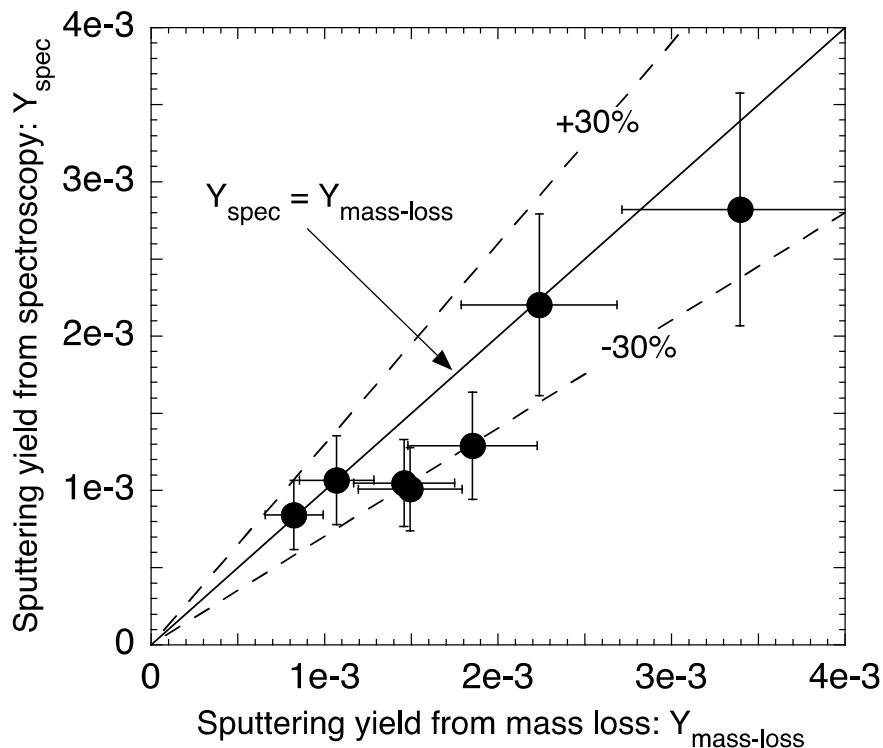
◆ $\Gamma_{\text{spt}}(\text{Cr})/\Gamma_{\text{spt}}(\text{Fe})$ is higher than the nominal bulk composition ratio (~ 0.088).

- Diffusion of Cr is faster than that of Fe.



Good agreement of sputtering yield between spectroscopy & mass loss verifies that our measured S/XB values are valid.

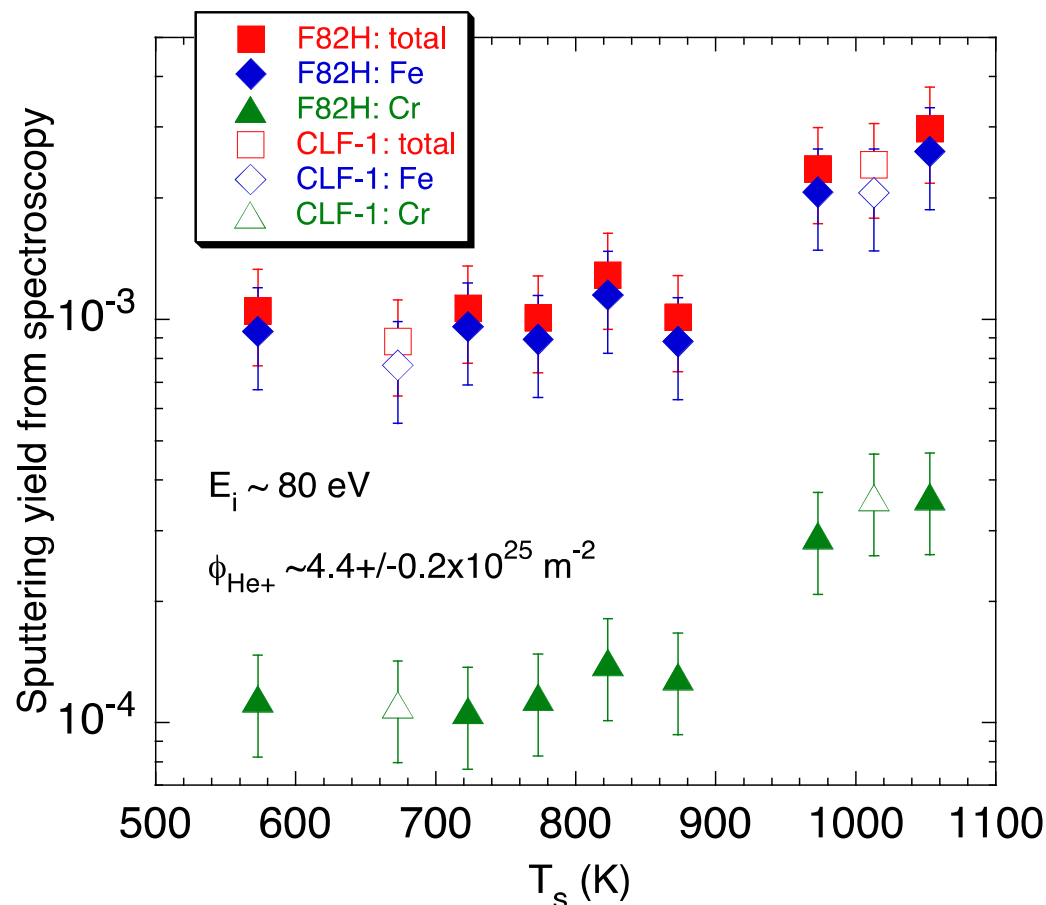
Comparison of the time- (fluence-) integrated F82H sputtering yields between the spectroscopic (Y_{spec}) and mass loss ($Y_{\text{mass-loss}}$) techniques.



The number of sputtered atoms from mass loss is calculated with the effective atomic mass (~55.5 amu) evaluated from spectroscopy.

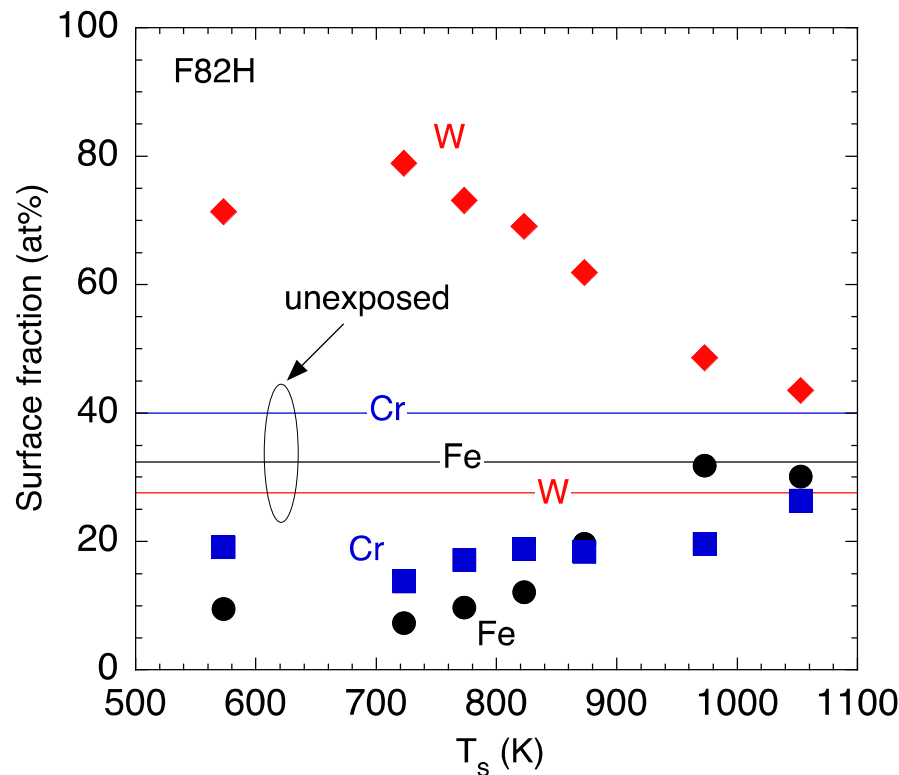
Sputtering yield is found to be constant up to $T_s \sim 900$ K, and to be enhanced at $T_s > 900$ K.

- ◆ He plasma exposure
 - $E_i \sim 80$ eV
 - $\phi_{\text{He}^+} \sim 4.4 \pm 0.2 \times 10^{25} \text{ m}^{-2}$
- ◆ $Y(\text{F82H}) \approx Y(\text{CLF-1})$
 - While the surface preparation is different between F82H (sanded) and CLF-1 (mirror-polished).

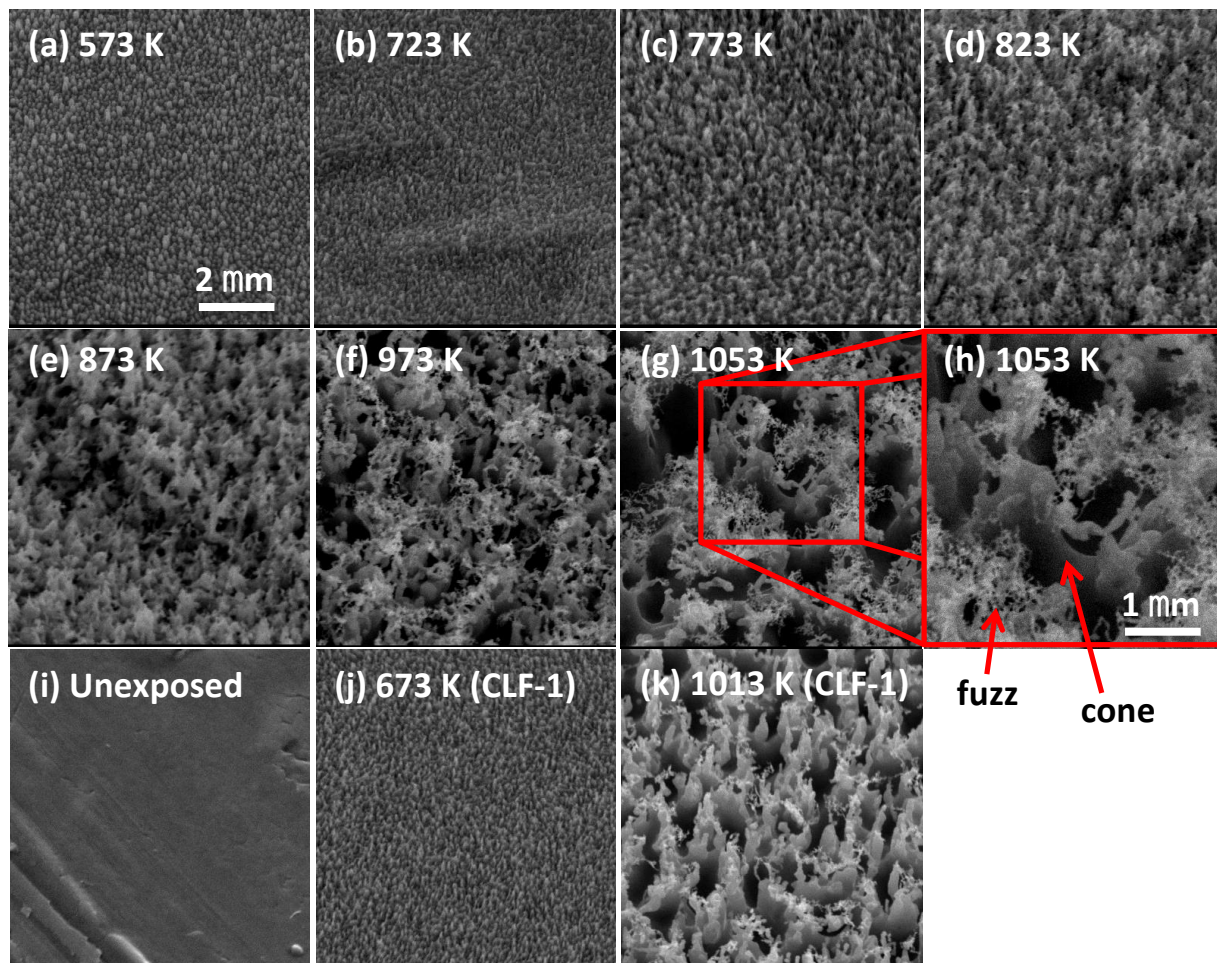


Surface enrichment of W due to preferential sputtering of Fe and Cr is confirmed with AES analysis.

- ◆ Fe may be preferentially removed by sanding, thus the surface composition of the unexposed surface strongly deviates from the bulk composition.
- ◆ The enrichment of W as well as the depletion of Fe and Cr are clearly seen, especially, at $T_s < 900$ K.
- ◆ The W enrichment is reduced at $T_s > 900$ K due presumably to the enhanced diffusion of Fe and Cr.



Cone-like structures become larger with increasing T_s , and W fuzz is formed on top of cones at $T_s \geq 973$ K.



In future fusion devices with RAFM steel first walls, T_s will need to be kept below 900 K from the sputtering point of view.

- ◆ S/XB values of Fe I 422.7 nm and Cr I 427.07 nm (425.4, 427.4, 428.9 nm) lines were experimentally determined for the first time.
 - Good agreement between Y_{spec} and $Y_{\text{mass-loss}}$ confirms that the measured S/XB values are valid.
 - This enables us to study sputtering properties of RAFM steels in more detail with spectroscopy.

- ◆ High-flux He plasma exposure to RAFM steels at low $E_i \sim 80$ eV leads to the reduction of the sputtering yield.
 - Preferential sputtering of Fe and Cr
 - ✧ Surface enrichment of W
 - Formation of sputter cone structures
 - ✧ W fuzz formation at $T_s \geq 973$ K on top

2. D retention properties of RAFM steels

Chemical composition (wt%) of RAFM steels as well as commercially available P92 FM steel

	Cr	W	V	Ta	C	Mn	Si	Ni
CLF-1	8.5	1.5	0.25	0.1	0.1	0.5	-	-
Eurofer	9	1.1	0.2	0.1	0.1	0.4	-	-
F82H	8	2	0.2	-	0.1	0.2	0.1	-
Rusfer	11	1.1	0.25	0.1	0.15	0.7	0.3	-
P92	8.5-9.5	1.5-2	0.15-0.25	-	0.07-0.13	0.3-0.6	≤ 0.5	≤ 0.4

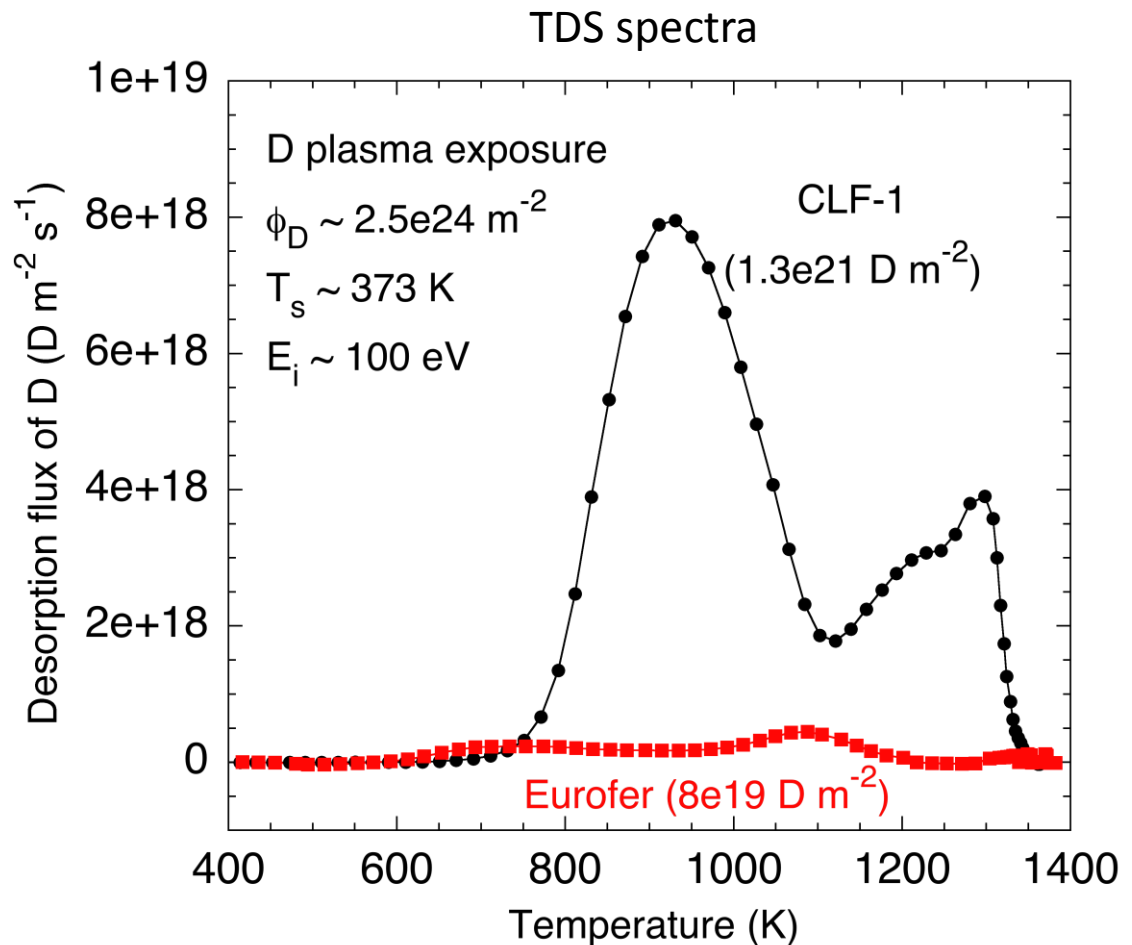
- Only elements with ≥ 0.1 wt%.
- P92 additionally contains Mo at 0.3-0.6 wt%.

- ◆ CLF-1, Eurofer, and F82H have been used in our experiments so far.
- ◆ But the number of these samples is very limited (no CLF-1 samples left).
- ◆ P92 may be used in future, since the composition of P92 is very similar to that of the RAFM steels.

D retention in CLF-1, Eurofer, and F82H RAFM steels were investigated under D plasma exposure in PISCES-A.

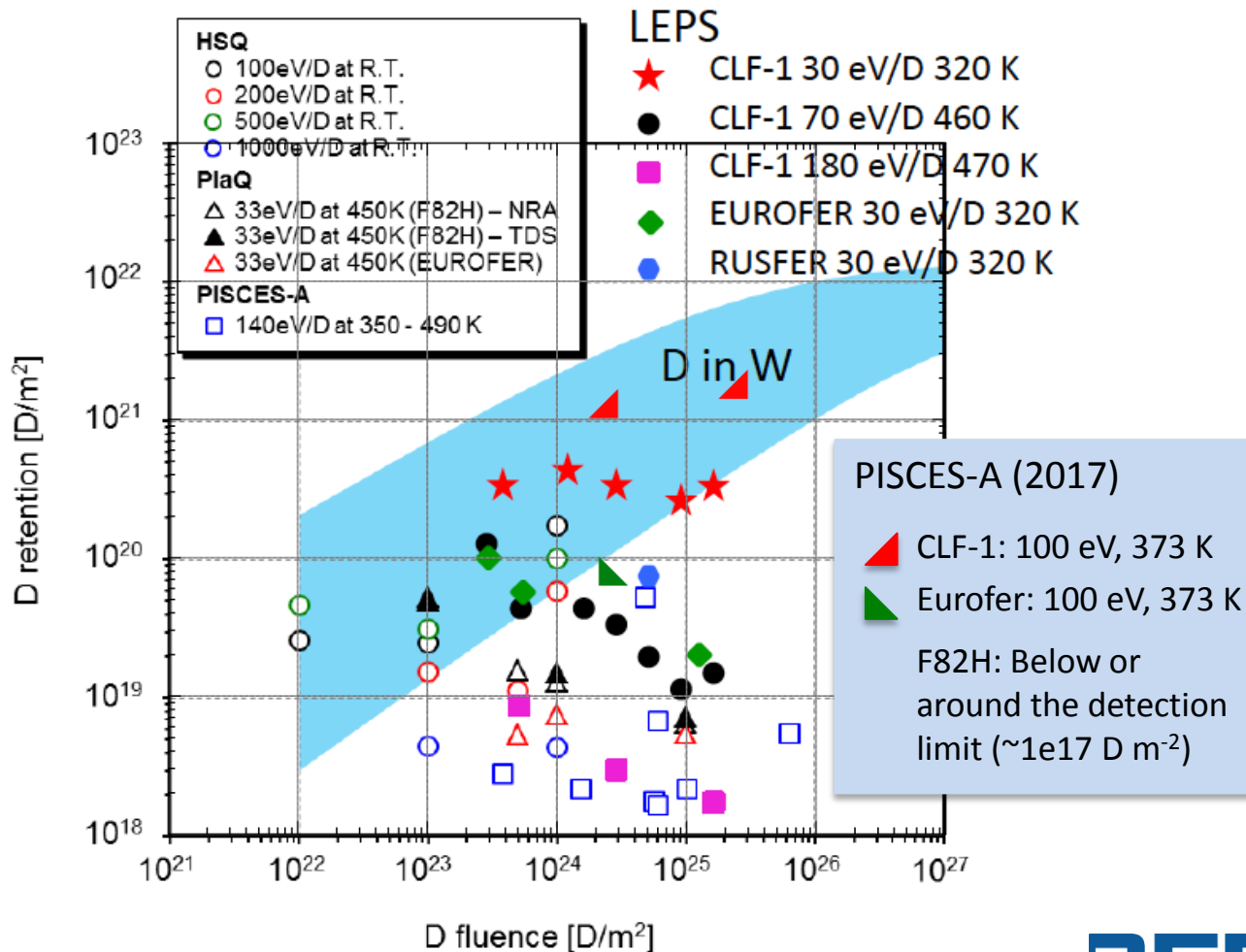
PISCES

- ◆ D plasma exposure
 - $\phi_D \sim 2.5e24 \text{ m}^{-2}$
 - $\Gamma_i \sim (2.5-3.5)e21 \text{ m}^{-2}\text{s}^{-1}$
 - $T_s \sim 373 \text{ K}$
 - $E_i \sim 100 \text{ eV}$
- ◆ Desorption flux of D is evaluated from both HD and D₂ signals.
- ◆ D retention in CLF-1 is much higher than that in Eurofer.
- ◆ D retention in F82H is much lower than CLF-1 and Eurofer, below or around the detection limit ($\sim 1e17 \text{ D m}^{-2}$).



PISCES-A (2017) data shows, Eurofer is consistent with others, while CLF-1 is higher than others.

Comparison of fluence dependence of D retention between W and RAFM steels (CLF-1, EUROFER and F82H)



◆ PISCES-A (2017) data does not decrease with increasing the fluence. (Need more data points, though.)

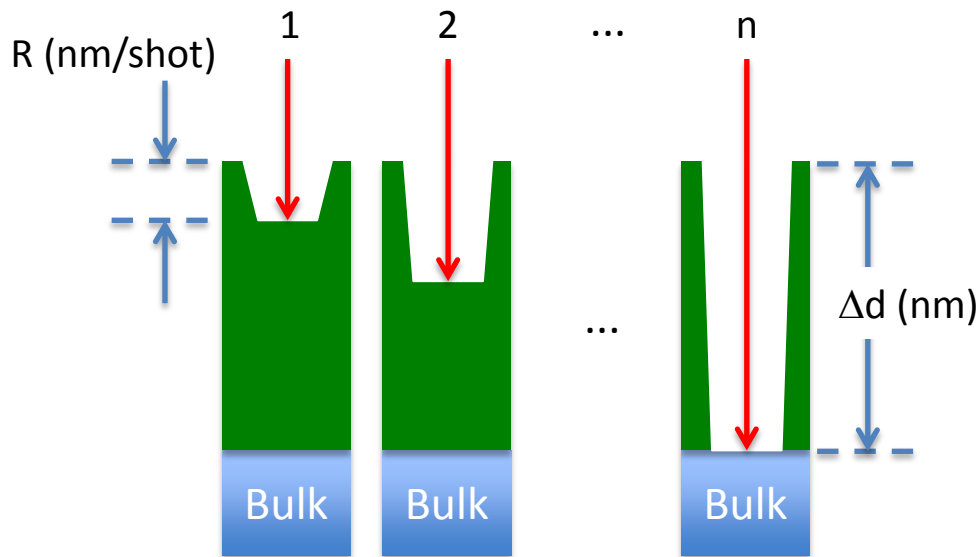
◆ Why does D retention decrease with increasing the fluence???

◆ Why is D retention in F82H very low in PISCES-A?

3. LIBS thickness measurement of layers thinner than ablation rate

- ◆ For a layer much thicker than the ablation rate

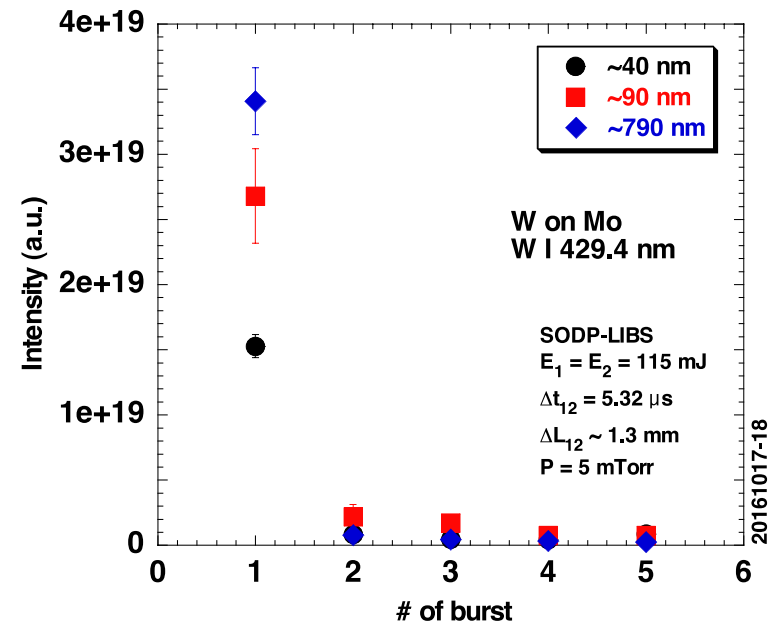
$$\Delta d \text{ (nm)} = R \text{ (nm/shot)} \times n$$



- This standard method **cannot be applied for a layer thinner than the ablation rate.**

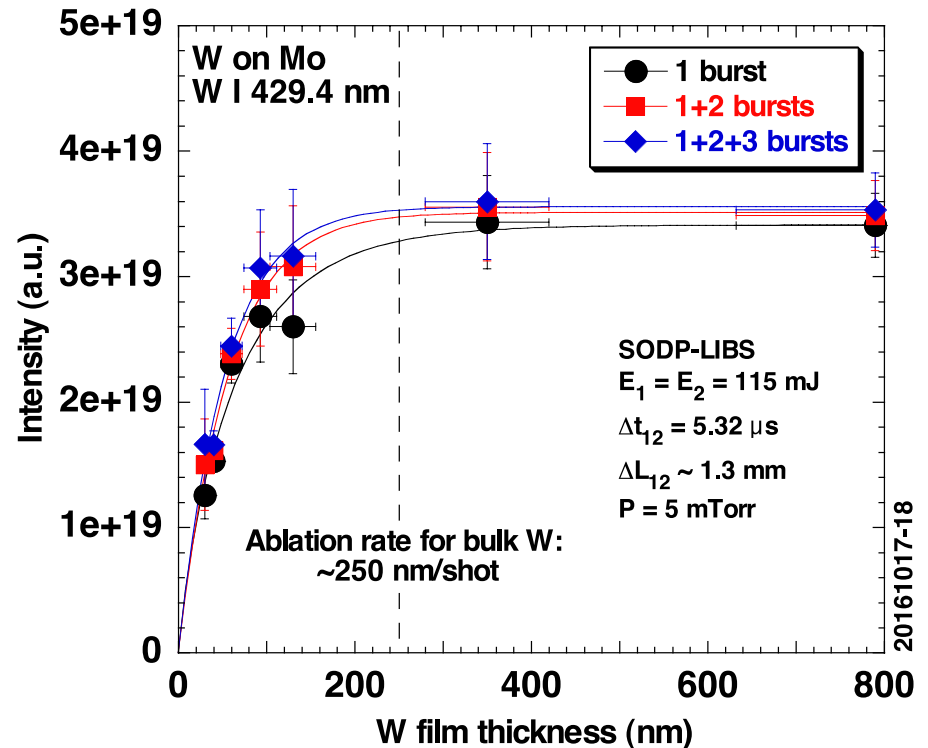
- ◆ Develop a new method to measure the thickness of a layer thinner than the ablation rate (less than a few hundred nm).

- The signal intensity increases with an increase in the layer thickness.



The new method utilizes the layer thickness dependence of the signal intensity as a calibration curve.

- ◆ The W I intensity depends strongly on the layer thickness up to around the ablation rate of bulk W.
- ◆ The film thickness can be obtained from the intensity below the ablation rate.
- ◆ Why does the intensity (I_{12} and I_{123}) saturate above the ablation rate?
- ◆ Fit function and coefficients



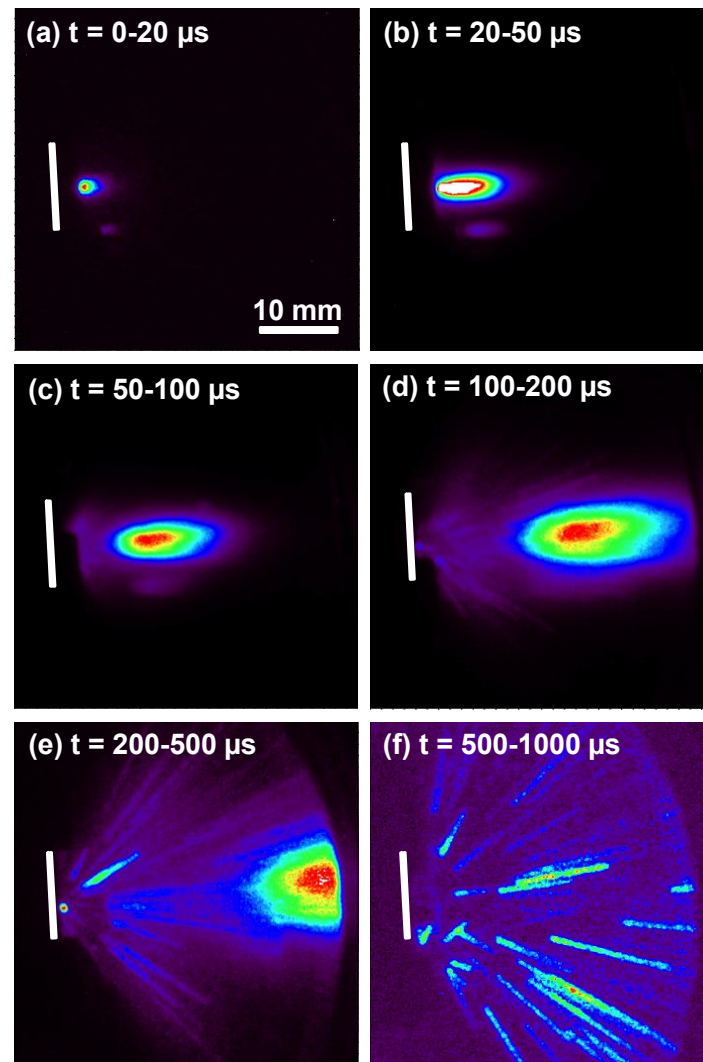
$$y = a(1 - \exp(-bx^c)).$$

	a	b	c	R
1 burst	$3.4e19 \pm 1.6e18$	$2.5e-2 \pm 1.7e-2$	0.88 ± 0.18	0.980
1 + 2 bursts	$3.5e19 \pm 8.2e17$	$1.6e-2 \pm 6.7e-3$	1.02 ± 0.11	0.994
1 + 2 + 3 bursts	$3.6e19 \pm 1.1e18$	$1.7e-2 \pm 9.6e-3$	1.02 ± 0.14	0.988

The underlying W layer below the ablated layer is significantly ejected as dust.

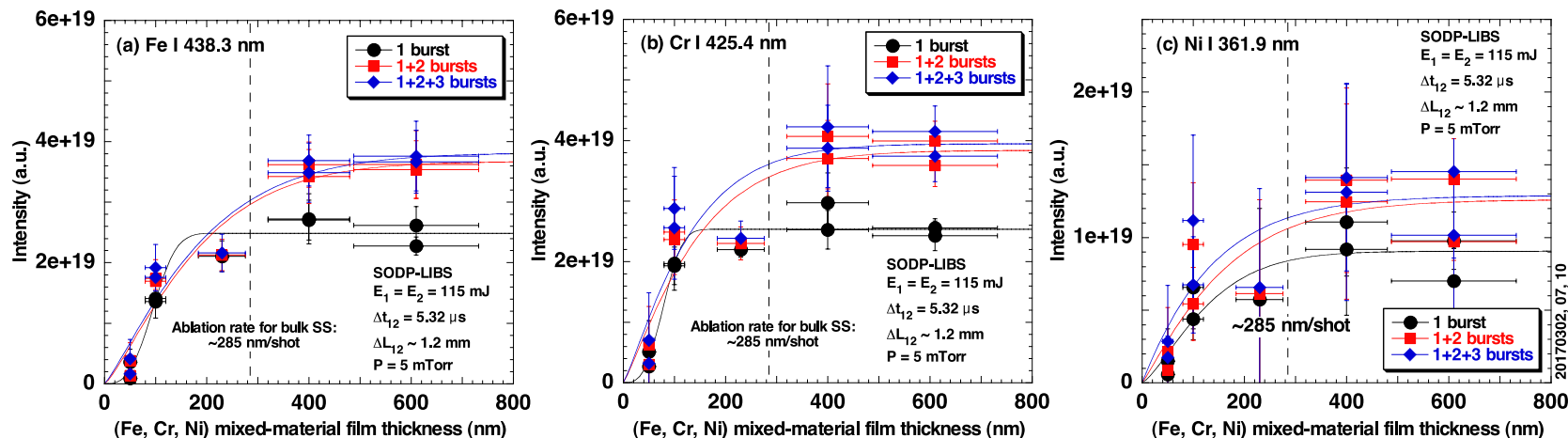
- ◆ The temporal evolution of ablated W plasma at the 1st burst was observed with an ICCD camera.
- ◆ Adhesion of the W layer to the mirror-polished Mo substrate may be weak.
- ◆ This can lead to the significant dust ejection.
- ◆ There was no W layer left after the 1st burst, and thus the W I intensity became very weak from the 2nd burst.

W layer ($\Delta d \sim 790$ nm) on Mo



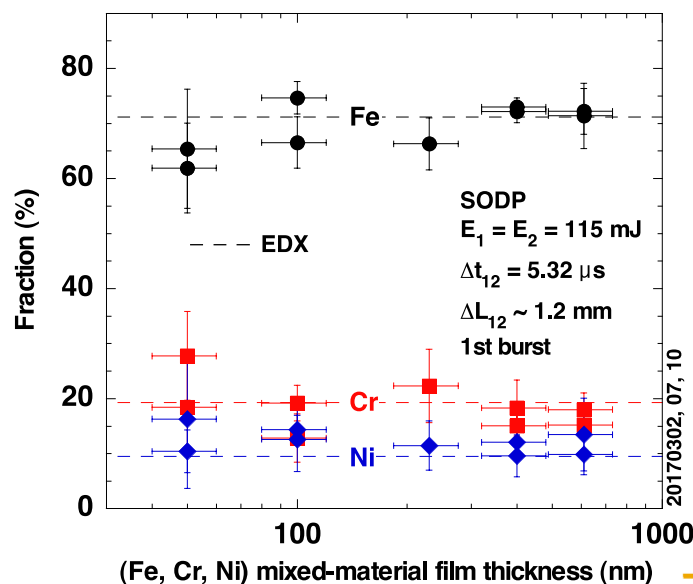
This new method also works with mixed-material layers.

◆ (Fe, Cr, Ni) mixed-material layers



◆ The composition of the multi-element layers is simultaneously derived with the calibration-free (CF) LIBS technique.

◆ The composition from LIBS agrees with that from EDX analysis.



◆ D retention properties of RAFM steels

- Investigate the fluence and temperature dependence
- Investigate effect of He mixture
- Use commercially available P92 FM steel as a surrogate?

◆ In-situ real-time LIBS surface analysis during plasma exposure

- Detect surface composition change due to preferential sputtering